PROCEEDINGS OF SPIE

SPIEDigitalLibrary.org/conference-proceedings-of-spie

Metasurface enhanced infrared spectroscopy using vertical nanostructures

Aditya Mahalanabish, Steven Huang, Gennady Shvets

Aditya Mahalanabish, Steven H. Huang, Gennady Shvets, "Metasurface enhanced infrared spectroscopy using vertical nanostructures," Proc. SPIE 12391, Label-free Biomedical Imaging and Sensing (LBIS) 2023, 123910H (16 March 2023); doi: 10.1117/12.2650689



Event: SPIE BiOS, 2023, San Francisco, California, United States

Metasurface enhanced infrared spectroscopy using vertical nanostructures

Aditya Mahalanabish, Steven H. Huang, Gennady Shvets*
School of Applied and Engineering Physics, Cornell University, Ithaca, New York, USA 14853
*Email: gs656@cornell.edu

ABSTRACT

Vertical nanostructures have been studied extensively and been reported to induce unique responses in cells, including the formation of clathrin coating and accumulation of actin filament which leads to cell membrane curvature around the nanostructures. In our previous works, we have demonstrated that arrays of plasmonic nanoantenna can be used as effective label free biosensors to study live cells when combined with IR spectroscopy in the reflection mode, known as metasurface enhanced IR spectroscopy (MEIRS). By fabricating these plasmonic metasurfaces on top of silica nanopillars, we demonstrate that we can expand the potential of MEIRS: increased protein IR absorption in the amide band and increased sensitivity of our biosensor to processes involving cellular interaction with vertical nanostructures.

Keywords: metasurface, IR spectroscopy, surface-enhanced infrared absorption, MEIRS, metasurface enhanced infrared absorption, vertical nanostructures

1. INTRODUCTION

Fourier Transform Infrared Spectroscopy (FTIR) is a non-invasive technique widely used for studying vibrational fingerprints of biological materials. Its application in studying biological samples have been exploited in the past to study non-homogeneous biological samples, such as monolayer of cells and tissues. However, conventional FTIR setup suffer from a few drawbacks which limit their application: mainly strong mid -IR light attenuation in water, weak molecular IR signal and thus long signal collection times. To get around these issues, designed plasmonic nanopatterned structures are used to enhance electromagnetic fields in hotspots and enhance molecular IR absorption via a process called Surface enhanced infrared absorption (SIERA). Periodic arrays of such resonant nanostructures have been engineered to have a tailored optical response over a broad range of frequencies and have been successfully applied in spectroscopic analysis of biomolecules like protein monolayers, lipid bilayers, dried and fixed cells. SIERA application can be extended to investigate live cells using such patterned resonant structures via a technique called metasurface enhanced IR reflection spectroscopy (MEIRS). Our group have previously demonstrated the use of MEIRS as a cellular assay technique to study responses of live cells to different chemical stimuli (proteases, chemotherapeutics) [1], as well as cholesterol depletion from cellular membrane by a chemical compound [2].

In recent years, vertical nanostructures have evolved as tools for cellular manipulation, to study live cell attachment and their response on surfaces with varying topography [3-6]. Nanotopographic features have been shown to incite unique chemical and physical responses in cell. One of the main physical responses to a nanotopographic surface is cell membrane curvature. Vertical nanostructures incite cells to undergo a process called clathrin mediated endocytosis (CME) which leads to the cell membrane wrapping around such structures by closely following the nanotopography on the surface.

In this work we combine MEIRS with vertical nanostructures to pave the way for an efficient tool for spectroscopically studying cellular adhesion and drug action in cells undergoing endocytocis and also put forth a method to increase FTIR signal-to-noise ratio compared to earlier flat metasurfaces. Cells grown on nanopatterned surfaces tend to wrap all around the projected metasurface (when on a nanopillar) instead of lying flat on top of a metasurface (in case of a flat substrate), leading to an increase in metasurface nearfield overlap with the cells. This leads to a stronger signal observed from the cells. Additionally, cell endocytosis also leads to accumulation of certain proteins like clathrin [5] and actin [6] around the region where the cell membrane curvature takes place (right where the metasurface is located). This phenomenon while increasing the amide signal observed by our MEIRS measurements will also make our technique very sensitive to processes which involve changes to the endocytic complex and cell-nanotopography interactions.

Label-free Biomedical Imaging and Sensing (LBIS) 2023, edited by Natan T. Shaked, Oliver Hayden, Proc. of SPIE Vol. 12391, 123910H · © 2023 SPIE 1605-7422 · doi: 10.1117/12.2650689

2. EXPERIMENTAL PROCEDURE

CaF₂ substrate of dimensions 12.5mm x 12.5mm x 0.5mm was coated with Silica thin film (~1um thickness) using plasma enhanced chemical vapor deposition (PECVD). Polymethyl methacrylate (PMMA) e-beam resist was spin coated on to the surface with the silica thin film and linear nanoantenna metasurface patterns were defined through e-beam lithography. Following this, 5nm Cr adhesion layer followed by 70nm Au layer and 18nm of Cr mask layer was evaporated on to the resulting structure. The metasurface pattern was transferred on to the Au layer through lift-off in an acetone bath. Next, we use reactive ion etch (with a mixture of CF₄ and Ar) to etch down the silica using the chromium layer as a hard mask. The silica is etched down to form nanopillars of varying heights (700nm, 850nm). For our measurements the fabricated gold nanoantenna had dimensions of 1.8um x 200nm. The array had a periodicity of 2.7um. Figure 1 (left) shows a schematic of the fabricated structure, with gold nanoantenna on raised silica pillars (3D metasurface) and 1(right) shows a scanning electron microscopy (SEM) image of the final fabricated metasurface. Figure 1 (left) shows a schematic of the fabricated structure and 1(right) shows a scanning electron microscopy (SEM) image of the final fabricated metasurface sample.

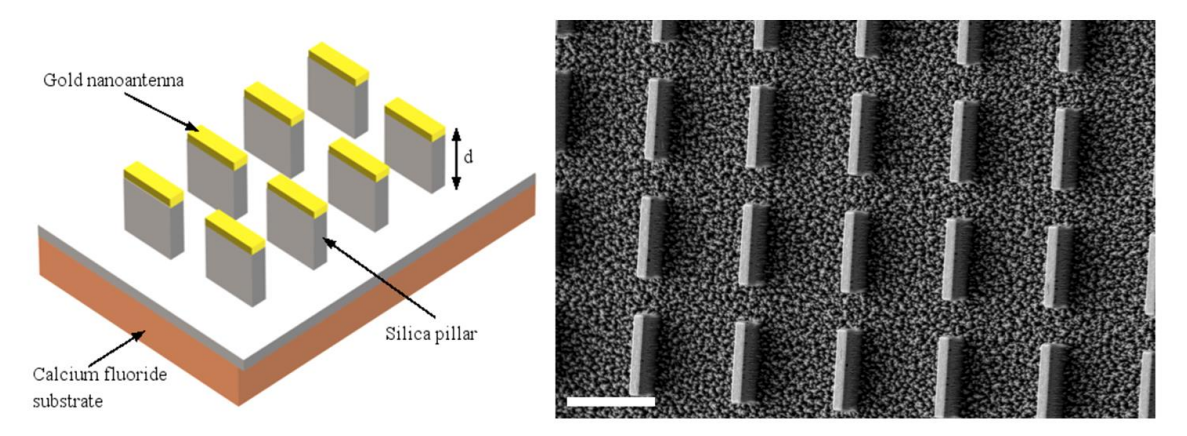


Figure 1: (left) Schematic of fabricated structure: vertical silica pillar with gold nanoantenna on top (3D metasurface); the height d of the pillar can be varied. (right) SEM image of the final fabricated structure when viewed at 35-degree angle; sample imaged here is 850nm tall and has a periodicity of 2.7um (Scale bar: 1um)

Before seeding the cells for measurement, the metasurface was sterilized with 70% ethanol, incubated overnight in $10 \, \mu \text{g/mL}$ fibronectin solution in Dulbecco's phosphate-buffered saline (DPBS) and washed with DPBS twice. Human epidermoid carcinoma cell line A431 cells were obtained from the American Type Culture Collection (ATCC) and cultured in Dulbecco's Modified Eagle Medium (DMEM) supplemented with $10 \, \%$ fetal bovine serum (FBS) and $1 \, \%$ penicillin-streptomycin. A431 cells were detached from culture flask using 0.25% trypsin-EDTA and seeded on the fibronectin-coated metasurface. The cells were incubated on the metasurface in DMEM + 10% FBS until confluent coverage (>95%) was achieved.

Schematic of the setup used for FTIR measurements on the fabricated samples is shown in figure 2. For our setup the samples are illuminated with an IR beam from the bottom. IR spectra were collected in reflection mode using Bruker Hyperion 3000 IR microscope with a 15X Cassegrain objective and a single element HgCdTe (MCT) detector, coupled with Bruker Vertex 70 Fourier Transform IR spectrometer. Unpolarized light was used for the measurement. Spectra were collected at 4 cm-1 resolution.

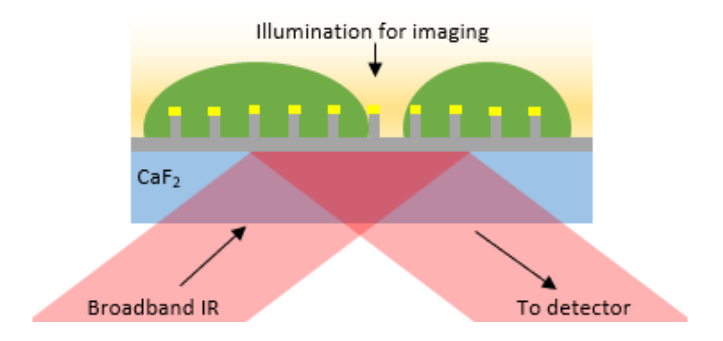


Figure 2: Schematic of the setup for optical measurements.

3. RESULTS

A431 cells grown on the fabricated 3D metasurface were fixed and dried for SEM imaging. Using a gallium Focused Ion Beam (FIB) we cut a cross-section through the substrate to get the image shown in figure 3. The cell can be seen to be wrapping around the pillar projections in and descending into the trenches between the nanopillars.

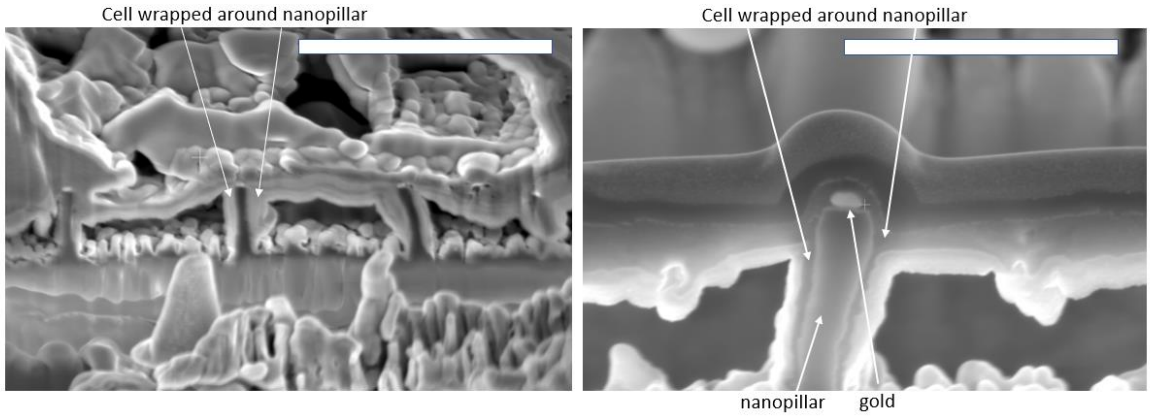


Figure 3: Cross-sectional images showing A431 cell wrapping around 850nm tall fabricated nanopillars (left) and corresponding close-up image (right)(Scale bar: left – 3um; right – 2um)

Figure 4 shows the reflectance spectra of A431 cells grown on gold nanoantennas on vertical nanopillars (3D nanoantennas) and compares them to the same cells grown on gold nanoantennas on flat substrates (2D nanoantennas). The gold nanoantenna is designed such that it's plasmonic resonance overlaps with that of the IR active Amide spectral region. The nanoantenna resonance peaks around $1650 \, \mathrm{cm}^{-1}$ for our design and as seen in figure 4 it overlaps with the broad water absorption dip around $1635 \, \mathrm{cm}^{-1}$. The difference in measured absorbance spectra with and without cells – referred to as the cell absorbance $A(\omega)$ – are plotted in figure 5 for 2D and 3D (700nm and 850nm tall nanopillar) nanoantennas. For the Amide II peak we observe an increase in signal by 1.6 (1.8) times for the 700nm (850nm) tall 3D nanoantennas compared with their 2D counterparts. The main factors leading to this increase in Amide II absorbance peak is increased near field overlap of wrapping cells, increased concentration of endocytic protein – especially clathrin and actin - around the projected nanopillar and transflectance. Transflectance refers to the phenomenon where light from the source is transmitted through the region with the silica pillars, scattered back from the resonant nanoantenna and travels thought the same region again before reaching the detector. This causes the light to travel twice through the cellular region wrapped around the silica pillars. It in turn helps probe into the cell body farther from the nanoantenna hotspots.

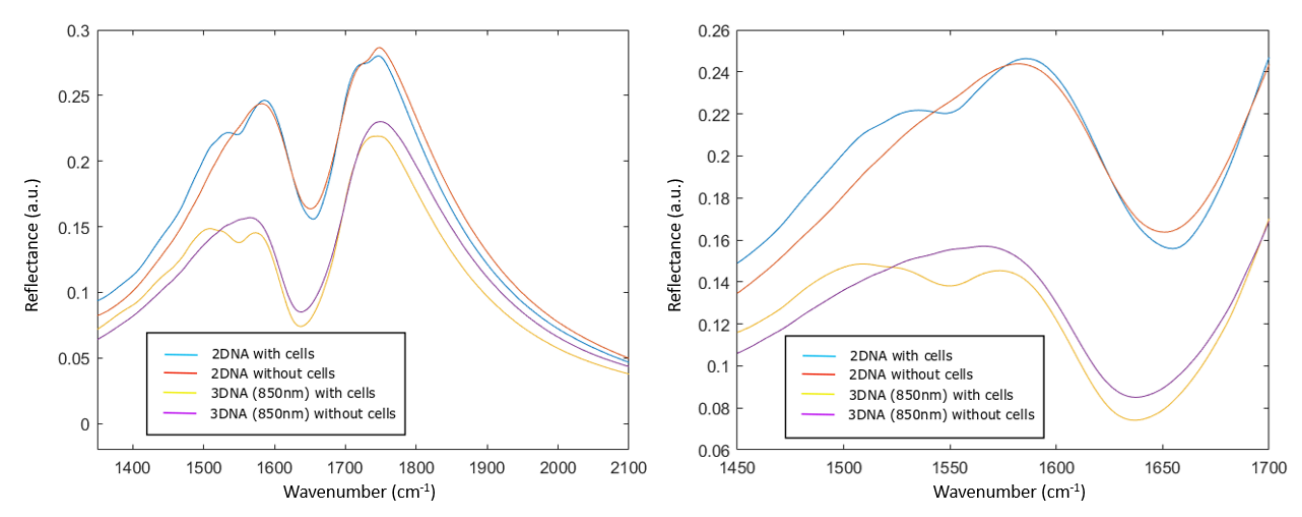


Figure 4: Reflectance spectra measured for the nanostructures in cell medium with (without) A431 cells grown on them. Nanostructures are either 2D or 3D (850nm tall). (Left) Zoomed-out and (right) zoomed-in spectra.

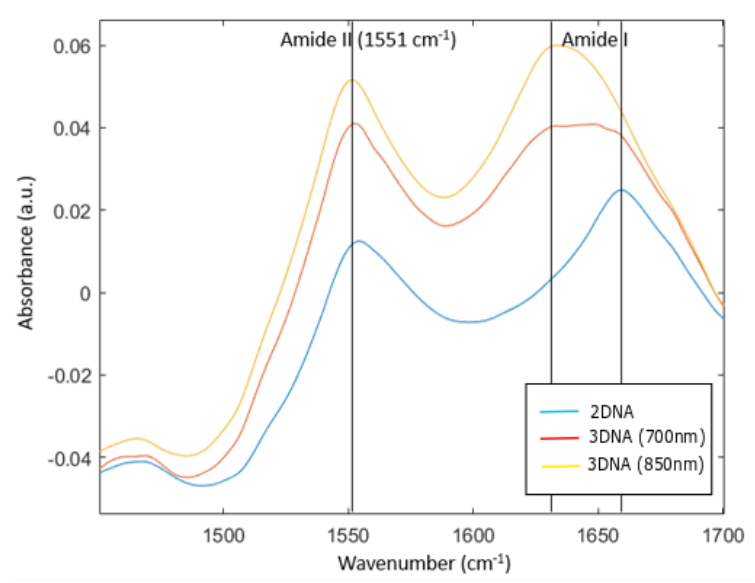


Figure 5: Comparison of differential absorbance for A431 cells grown on 2D nanoantenna metasurface with that grown on 3D nanoantenna (700nm and 850nm tall nanopillar) metasurfaces (Differential absorbance: log₁₀ [Reflectivity of cell grown on metasurface/Reflectivity of metasurface in cell medium])

We also observe a clear difference in the Amide I region for 2D vs 3D nanoantennas. The amide I peak appears to be broadened for the nanopillar structures when compared to the 2D case. To get a clearer image of the Amide I sub peaks, we take second derivative of the differential absorbance in figure 5. In figure 6 we see two Amide I sub-peaks (1631 cm⁻¹ and 1656 cm⁻¹) can be seen in the case of the nanopillar samples (700nm, 850nm tall nanopillars), compared to the single peak (1656cm⁻¹) in the case of the flat substrate. The 1656 cm⁻¹ peak that can be seen in both types of samples is associated with proteins having alpha helix secondary structures [7]. The 1631 cm⁻¹ peak which is observed in the nanopillar samples only is associated with proteins having beta sheets secondary structures [6]. Our current hypothesis for the 1631 cm⁻¹ peak in the nanopillar case is that it appears because of the protein composition in the CME complex, which is responsible for the membrane curvature around the nanoantennas. AP2 adaptor proteins, which are responsible for the attachment of clathrin on the cell membrane, is made up of 44% beta sheets [8], which is much higher than most other proteins found near the cell membrane; for example, F-actin which forms the cellular cytoskeleton is made of some nominal 4% beta sheets [9].

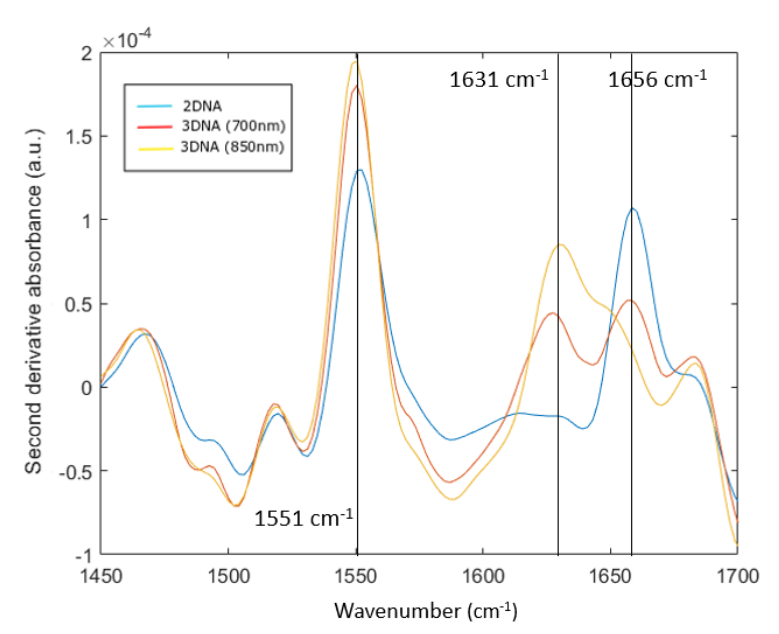


Figure 6: Second derivative spectra obtained from the differential absorbance in figure 5 above, for the cases of 2D nanoantenna metasurface and 3D nanoantenna (700nm and 850nm nanopillar) metasurfaces.

4. CONCLUSION

In conclusion we integrated MEIRS with vertical nanopillars and observed the differences in cellular spectra compared to a flat 2D metasurface. The 3D metasurface showed enhanced Amide II absorbance as a result of a few different factors: cellular wrapping increasing field overlap, endocytic protein concentration around nanoantennas and transflectance. The 3D metasurface also shows a difference in the Amide I spectral region associated with protein secondary structure of endocytic proteins. This proof-of concept experiment shows that MEIRS can indeed be used to study live cells attached on nanotopographic surfaces other than flat surface. In addition to probing cellular processes near the cell membrane via plasmonic near fields, combining MEIRS with vertical nanostructures opens up a way to look deeper into the cell via transflectance.

ACKNOWLEDGEMENT

The research reported here was supported by the National Cancer Institute of the National Institutes of Health under award number R21 CA251052 and by the National Institute of General Medical Sciences of the National Institutes of Health under award number R21 GM138947. This work was performed in part at the Cornell NanoScale Facility, a member of the National Nanotechnology Coordinated Infrastructure (NNCI), which is supported by the National Science Foundation (Grant NNCI-2025233). This work made use of the Cornell Center for Materials Research Shared Facilities which are supported through the NSF MRSEC program (DMR-1719875).

REFERENCES

- [1] Shen P-T, Huang SH, Huang Z, Wilson JJ, Shvets G. Probing the Drug Dynamics of Chemotherapeutics Using Metasurface-Enhanced Infrared Reflection Spectroscopy of Live Cells. *Cells*; 11(10):1600. (2022)
- [2] Huang, S. H. *et al* Monitoring the eefects of chemical stimuli on live cells with metasurface enhanced infrared reflection spectroscopy. *Lab Chip*, **21**, 3991 (2021)
- [3] Li, X., Matino, L., Zhang, W. et al. A nanostructure platform for live-cell manipulation of membrane curvature. *Nat Protoc* 14, 1772–1802 (2019)
- [4] Vinje, J.B., Guadagno, N.A., Progida, C. et al. Analysis of Actin and Focal Adhesion Organisation in U2OS Cells on Polymer Nanostructures. *Nanoscale Res Lett* 16, 143 (2021)
- [5] Zhao, W., Hanson, L., Lou, HY. et al. Nanoscale manipulation of membrane curvature for probing endocytosis in live cells. *Nature Nanotech* 12, 750–756 (2017)
- [6] Lou HY., Zhao W., Xioa L. et al. Membrane curvature underlies actin reorganization in response to nanoscale surface topography. *Proceedings of the National Academy of Sciences* 116 (46) 23143-23151 (2019)
- [7] Yang, H., Yang, S., Kong, J., Dong, A., & Yu, S. Obtaining information about protein secondary structures in aqueous solution using Fourier transform IR spectroscopy. *Nature Protocols*, 10(3), 382–396 (2015)
- [8] Owen, DJ., Vallis, Y., Pearse, B.M.F., McMahon, H.T. The structure and function of b2-adaptin appendage domain. *EMBO Journal* 19:4216-4227 (2000)
- [9] Dominguez R, Holmes KC. Actin structure and function. Annu Rev Biophys. 2011;40:169-86 (2011)